

# Complex Couplings - A Universal, Adaptive, and Bilinear Formulation of Power Grid Dynamics

Anna Büttner<sup>\*</sup> and Frank Hellmann<sup>†</sup>

*Potsdam Institute for Climate Impact Research, Potsdam 14473, Germany*

 (Received 30 October 2023; revised 12 December 2023; accepted 5 January 2024; published 7 February 2024)

The energy transition introduces new classes of dynamical actors into the power grid. There is, in particular, a growing need for so-called grid-forming inverters (GFIs) that can contribute to dynamic grid stability as the share of synchronous generators decreases. Understanding the collective behavior and stability of future grids, featuring a heterogeneous mix of dynamics, remains an urgent and challenging task. Two recent advances in describing such modern power grid dynamics have made this problem more tractable. First, the normal form for grid-forming actors provides a uniform technology-neutral description of plausible grid dynamics, including grid-forming inverters and synchronous machines. Second, the notion of the complex frequency has been introduced to effortlessly describe how the nodal dynamics influence the power flows in the grid. The major contribution of this paper is to show how the normal-form approach and the complex-frequency dynamics of power grids combine and how they relate naturally to adaptive dynamical networks and control-affine systems. Using the normal form and the complex frequency, we derive a remarkably elementary and universal equation for the collective grid dynamics. Notably, we obtain an elegant equation entirely in terms of a matrix of complex couplings, in which the network topology does not appear explicitly. These complex couplings give rise to new adaptive network formulations of future power grid dynamics. We give a new formulation of the Kuramoto model, with inertia as a special case. Starting from this formulation of the grid dynamics, the question of the optimal design of future grid-forming actors becomes treatable by methods from affine and bilinear control theory. We demonstrate the power of this perspective by deriving a quasilocal control dynamics that can stabilize arbitrary power flows, even if the effective network Laplacian is not positive definite.

DOI: [10.1103/PRXEnergy.3.013005](https://doi.org/10.1103/PRXEnergy.3.013005)

## I. INTRODUCTION

Due to the energy transition, conventional power plants are being replaced by renewable energy sources (RESs) such as wind and solar photovoltaics. RESs are predominantly connected to the power grid via power electronic inverters. Furthermore, power electronic interfaces are also in use for many loads and for connecting storage solutions such as batteries to power grids. Currently, most inverters are grid following and have to rely on a stable grid to function. However, as we move toward a fully renewable grid, there is a growing need for so-called grid-forming

inverters [1] (GFIs) that can contribute to the grid stability independent of conventional generation.

Popella *et al.* have shown that following one of the scenarios in the German Network Development Plan [2], more than 80% of all inverters installed from 2021 need to be grid forming to assure a stable power grid in 2035 [3]. This shift presents a significant challenge, as GFIs are a relatively new and complex technology, of which there is a limited practical and theoretical understanding. In future grids, these GFIs will coexist with a much-reduced number of conventional generators. The collective dynamics of such inverter-dominated networks remain a challenging topic [4].

For almost all proposed types of GFIs, there is an analysis of the stability of the individual machine. The stability of the entire network, however, is rarely addressed, with Refs. [5,6] as notable exceptions. Most research on the collective behavior of the power grid is still based on the paradigmatic Kuramoto model [7]. For generators, we already know, from the study of higher-order models that include voltage dynamics, that the Kuramoto model can be misleading, for the individual dynamics [8] but also

<sup>\*</sup>buettner@pik-potsdam.de

<sup>†</sup>hellmann@pik-potsdam.de

*Published by the American Physical Society under the terms of the [Creative Commons Attribution 4.0 International](https://creativecommons.org/licenses/by/4.0/) license. Further distribution of this work must maintain attribution to the author(s) and the published article's title, journal citation, and DOI.*

for the collective phenomena [9]. As we move toward an inverter-dominated grid, we even lack the consensus on higher-order models of GFIs, as vastly different realizations of grid-forming capabilities are possible. However, important phenomena occurring in inverter-dominated networks cannot be captured by the Kuramoto model.

To study collective phenomena in heterogeneous systems, a description of all grid-forming actors, conventional and future GFI-based, is needed. Kogler *et al.* [10] address this, by introducing the normal form, a dynamic technology-neutral formulation for the dynamics of grid-forming actors. This normal-form approach provides a concise and meaningful parametrization of the space of plausible power grid actors, especially when they are near their desired operational state. Thus, it is well suited to the study of power systems with a heterogeneous mix of dynamical actors.

Independently, Milano has recently introduced the notion of the complex frequency [11] to elegantly describe how the nodal dynamics influence the power flows in the grid.

In this paper, we show that the two formulations introduced above complement each other perfectly. Combining their respective insights, we introduce new dynamical variables, termed complex couplings (Sec. III A), that describe the evolution of the power grid completely. The complex coupling immediately gives rise to an adaptive network formulation for general power grid dynamics (see Sec. II D). As a special case, in Sec. III B, we derive the Kuramoto model with inertia in this formulation. Further, in Sec. III C, we derive a new and surprisingly elegant formulation of the collective grid dynamics. This formulation has the remarkable property that the network adjacency matrix no longer appears explicitly in the equations but is encoded in the initial condition.

Furthermore, we show by using the complex frequency and complex couplings that tracking problems for the power and voltage magnitude can be stated as so-called bilinear control problems (see Secs. II E and IV). Solving this problem under the constraint of a fully decentralized controller using only local information is challenging. However, the formulation provides a natural quasiloal Lyapunov-function controller, which we introduce in Sec. IV D, which is globally synchronizing while reducing the tracking error.

A major contribution of this paper is to systematically collect and describe the various ways in which complex-frequency dynamics of power grids, normal-form descriptions of grid-forming actors, and concepts from control theory and dynamical systems intersect. To provide the reader with a background to the relevant fields, we will begin by recalling the most relevant concepts from power grids, adaptive dynamical networks, and bilinear control systems in Sec. II. Then, in Sec. III A, we will introduce

the new formulations of the grid dynamics. Finally, we will explore the control aspects in Sec. IV. We also provide an appendix with various useful related calculations.

## II. THEORETICAL BACKGROUND

### A. Balanced ac power grid variables

Generally, power grids consist of several parallel circuits carrying phase-shifted ac voltages and currents. We will focus on the typical case of three phases. A three-phase voltage signal  $V_1$ ,  $V_2$ , and  $V_3$  is called balanced if it satisfies  $V_1 + V_2 + V_3 = 0$  at all times. Balanced signals can be expressed in terms of a rotating two-dimensional vector, often referred to as the  $dq$  coordinates [12]. Defining the complex voltage state  $v = v_d + jv_q$ , also called the Park vector, we can write the original signal as  $V_l = \text{Re}(\exp(jl/3\pi)v)$ , where  $l$  denotes the different phases. The complex voltage  $v$  can be written in terms of the phase  $\theta$  and amplitude  $V_m \geq 0$ , as

$$v(t) = V_m e^{j\theta}. \quad (1)$$

Note that, with our definition, the amplitude  $V_m$  is the (peak) voltage magnitude of the three-phase signal. As we will assume balanced conditions throughout, the Park vector  $v(t)$  captures the full state space of the system. The same procedure is used to express the three-phase currents in terms of a single complex current  $i(t)$ .

It is then a straightforward calculation to see that the real part of  $v\bar{i}$  is  $\frac{3}{2}$  times the instantaneous power contained in a three-phase current  $i$  at voltage  $v$ . The imaginary part is called the instantaneous reactive power and is interpreted as the amount of energy that is injected into the transmission line without flowing through it. The full quantity  $S_c = \frac{2}{3}v\bar{i}$  is called the complex power. In what follows, we will absorb the factor  $\frac{2}{3}$  into the coefficients and abuse terminology slightly to speak simply of

$$S = P + jQ = v\bar{i} \quad (2)$$

as the complex power.

### B. Complex frequency

The frequency  $f$  is the most important variable for operating, controlling, and monitoring power grids [12]. According to the accepted IEEE standard [13], the frequency  $f(t)$  of a signal  $x(t)$  with amplitude  $X_m$  and phase  $\theta$  is defined as

$$x(t) = X_m(t) \cos(\theta(t)), \quad (3)$$

$$f(t) = \frac{1}{2\pi} \dot{\theta}(t). \quad (4)$$

This standard definition of frequency in ac power grids is only meaningful when a state with slowly varying amplitude is assumed. However, in power grids, fast amplitude changes in the voltage are possible. This standard definition cannot distinguish between phase and amplitude variations in a meaningful way. The objective of the complex frequency, which has been introduced in Ref. [11], is to overcome this issue by providing an interpretation of the instantaneous frequency as a state-space velocity. As long as it is nonzero, we can consider the time derivative of the logarithm of the voltage  $v(t)$  given in Eq. (1):

$$v(t) = e^{\ln(V)+j\theta} = e^{\sigma+j\theta}, \quad (5)$$

$$\eta := \dot{\sigma} + j\dot{\theta} = \rho + j\omega, \quad (6)$$

$$\dot{v}(t) = (\dot{\sigma} + j\dot{\theta})v = (\rho + j\omega)v = \eta v, \quad (7)$$

where  $\theta$  is again the phase of the voltage and  $\sigma$  is the logarithm of the voltage magnitude  $V$ .  $\omega$  is the angular velocity of the signal and  $\rho$  is the rate of change of the log-voltage amplitude. The complex number  $\eta$  is defined as the complex frequency [11]. For slowly changing amplitudes, where both definitions are applicable, the standard definition of the frequency coincides with the imaginary part of the complex frequency.

The complex frequency has already found numerous applications, ranging from the inertia estimation of virtual power plants [14] to analyzing the linear [15] and nonlinear stability [16] of networks that are composed of dispatchable virtual oscillators [17], a proposed type of GFI. Furthermore, Ref. [18] shows the connection between the complex frequency and power for several different converter controllers, including GFIs.

The authors of Ref. [15] introduce complex-frequency synchronization, a novel concept of synchronization. Equation (6) shows that to obtain full synchrony of the voltages, both the angular frequency and the rate of change of voltage have to match. During rate-of-change-of-voltage synchronization, the voltage amplitudes are still allowed to change but at the same exponential rate.

### C. Normal form

The authors of Ref. [10] have introduced the normal form, a technology-neutral formulation for the dynamics of grid-forming actors. The main result of Ref. [10] is that the symmetry under global phase shifts of the nodal dynamics can be exploited to formulate the dynamics in terms of invariants of the symmetry. The entire interaction between grid-forming actors and the grid can be written in terms of the active power  $P$  and the reactive power  $Q$ , as well as the square of the voltage magnitude  $v = v\bar{v}$ , which form an elegant complete set of invariants for power grids.  $P$ ,  $Q$ , and  $v$  are exactly the quantities needed to describe the desired behavior of grid-forming actors, as these are responsible for balancing the active power and

providing enough reactive power to maintain the nominal voltage levels. Following Ref. [10], the dynamical behavior of grid-forming actors can be generally written in the following form:

$$\dot{v} = v g^v(v, P, Q, x_c), \quad (8)$$

$$\dot{x}_c = g^{x_c}(v, P, Q, x_c), \quad (9)$$

where  $v$  is again the complex voltage,  $x_c$  are the internal dynamics of the control of the grid-forming actors, and  $g^v$  and  $g^{x_c}$  are differentiable, potentially nonlinear, functions. Using the complex frequency given in Eq. (7), we see that we can rewrite the first equation simply as

$$\eta = g^v(v, P, Q, x_c), \quad (10)$$

which gives the dynamics a novel interpretation. By definition, the complex frequency  $\eta = \dot{v}/v$  determines the voltage dynamics. As  $\eta$  is invariant under global phase shifts, it can only depend on other invariants if the entire system is to be invariant. In particular,  $\eta$  cannot depend explicitly on  $v$ .

### D. Adaptive dynamical networks

Adaptive dynamical networks are a class of systems that change their coupling  $K_{hm}(t)$ , between node  $h$  and  $m$ , over time depending on the dynamical state  $y_h$  of the nodes of the network. The review paper of Ref. [19] gives an excellent overview of the applications, dynamical phenomena, and available mathematical methods for adaptive dynamical networks. Furthermore, Ref. [20] features a rundown of the concept of adaptivity and how it applies across different scientific disciplines. In this work, we will focus on weighted adaptive dynamical networks that are in general defined as follows:

$$\dot{y}_h = f_h(y_h) + \sum_{m=1}^M K_{hm} \gamma(y_h, y_m), \quad (11)$$

$$\dot{K}_{hm} = H(K_{hm}, y_h, y_m), \quad (12)$$

where  $f_h$  describes the local dynamics of node  $h$ ,  $\gamma$  is the coupling function, and  $H$  is the adaptation function.

Recently, it has been revealed that dynamical power grid models, based on phase-oscillator models, are connected to adaptive networks [21]. In particular, it has been shown that the Kuramoto model with inertia and the Kuramoto model with inertia and voltage dynamics [22], in electrical engineering referred to as a third-order machine model [8], can be written as a system of adaptively coupled phase oscillators. Using this approach, the voltage dynamics can be interpreted as an additional adaptivity term. It has been shown that phase-oscillator models and oscillators on adaptive networks share many different dynamical phenomena, such as solitary states [21,23].

In this work, we will introduce a type of complex coupling  $K_{hm}$  that allows us to represent general dynamical power grid models as adaptive networks as long as the complex frequency  $\eta$  is well defined.

### E. Bilinear and control-affine systems

Power grids are inherently nonlinear systems. Therefore, to control them, nonlinear control theory is required, with all its associated difficulties. A linear approximation [24] of the system could be used instead, but then nonlinear effects could not be taken into account and the controller would have limited effectiveness. A relatively novel alternative to traditional model-based techniques are data-driven control methods that do not require explicit models for the system to be controlled. For example, data-enabled predictive control has been introduced in Ref. [25] and can be used to compute optimal and safe control policies. Furthermore, the authors of Ref. [26] have recently introduced a model-free method that allows tracking control of complex trajectories using machine learning.

The complex-frequency and normal-form equations reveal that the power grid can be interpreted as a system in which the control variable is linear. Such systems are called control-affine systems [27] and are of the form

$$\dot{\mathbf{y}} = \mathbf{F}(\mathbf{y}) + \mathbf{G}(\mathbf{y})\mathbf{u}, \quad (13)$$

where  $\mathbf{y}$  and  $\mathbf{u}$  are the state and control vectors, respectively.  $\mathbf{F}(\mathbf{y})$  and  $\mathbf{G}(\mathbf{y})$  are possibly nonlinear functions.

The power grid equations that we will find (see Sec. IV) are bilinear systems [28], meaning that  $\mathbf{F}(\mathbf{y})$  and  $\mathbf{G}(\mathbf{y})$  are linear functions of  $\mathbf{y}$ . This leads to the bilinear form of the control system:

$$\dot{y}(t) = \sum_{a=1}^A u_a(t) N_a y(t), \quad (14)$$

where  $y$  and  $u$  are again the state and control, respectively, and  $N_a$  are the system matrices.

Bilinear systems are an area of intensive research, as they occur in various contexts [29], such as nuclear reactors. There is considerable work on bilinear control systems [28]. Below, we will see that exploiting the control-affine structure already allows us to derive interesting new control laws.

## III. NEW POWER GRID EQUATIONS

We begin by introducing the dynamics of the complex coupling, before deriving new adaptive formulations of power grids.

### A. Complex-coupling dynamics

In Ref. [11], Milano considers the dynamics of the complex power  $S_h$  in terms of a dynamical-coupling term. In

Milano's paper, these coupling terms are referred to as  $s_{hm}$ . To avoid confusion with the power flows on the lines, we will use  $K_{hm}$  in this work. Take  $Y_{hm} = 1/Z_{hm}$  as the admittance on the line connecting nodes  $h$  and  $m$ . We then introduce the admittance-weighted graph Laplacian  $L_{hm}$  as

$$L_{hm} = -Y_{hm} + \delta_{hm} \sum_k Y_{hk}, \quad (15)$$

where  $\delta_{hm}$  is the Kronecker delta. The dynamical-coupling terms  $K_{hm}$ , which will play the role of the adaptive coupling in the sense of Eq. (12), are defined as

$$K_{hm} = v_h \bar{L}_{hm} \bar{v}_m, \quad (16)$$

where  $\bar{L}_{hm}$  is the complex conjugate of the Laplacian. These coupling terms  $K_{hm}$  do not have a physical interpretation but they have the important property that

$$S_h = \sum_m K_{hm} \quad (17)$$

holds, as

$$i_{hm} = Y_{hm}(v_h - v_m), \quad (18)$$

$$i_h = \sum_m i_{hm} = \sum_m L_{hm} v_m, \quad (19)$$

$$S_h = v_h \bar{i}_h = \sum_m v_h \bar{L}_{hm} \bar{v}_m = \sum_m K_{hm}. \quad (20)$$

Using the voltage dynamics in Eq. (7), the dynamics of the coupling are given by

$$\dot{K}_{hm} = (\eta_h + \bar{\eta}_m) K_{hm}. \quad (21)$$

Thus the dynamics for the nodal complex power  $S_h$  are given by

$$\dot{S}_h = \eta_h S_h + \sum_m K_{hm} \bar{\eta}_m, \quad (22)$$

which is Eq. (32) in Ref. [11]. The diagonal coupling terms  $K_{mm}$  describe the evolution of the square of the local voltage magnitude  $v_m$  up to a constant factor:

$$v_m = v_m \bar{v}_m = \frac{K_{mm}}{\bar{L}_{mm}} = \frac{K_{mm}}{\sum_h \bar{Y}_{mh}}. \quad (23)$$

From Eq. (21), we can see that the system has two possible sets of fixed points. The first set of fixed points coincides with  $K_{hm} = 0$ , which can either be achieved when  $h$  and  $m$  are not connected by a transmission line or when there is a total voltage collapse at either node. The second type of fixed point is defined by  $\eta_h = -\bar{\eta}_m$  throughout the connected component. If the system is connected at the fixed

point, i.e., for every two nodes there is a walk of nonzero  $K_{hm}$  connecting them, then this implies that  $\eta_h = j\omega_{\text{global}}$  for all  $h$ .

This shows an immediate advantage of considering a dynamical system given entirely in terms of invariants, the desirable operating states are fixed points rather than limit cycles, which simplifies system identification and control synthesis considerably. The stability of the synchronous fixed points can now be expressed using a master stability function [30], an approach that has recently been extended to a large class of adaptive networks [31].

Following Ref. [11], we assume that the transmission line dynamics are faster than the nodal dynamics and that a quasi-steady-state model can be employed for the transmission lines. In Appendix B, we show briefly how to extend this description to more realistic line models. Furthermore, we point out that a similar, albeit less concise, formulation can be achieved in power-flow variables. The derivation can be found in Appendix C.

The coupling dynamics in Eq. (21) can be used to rewrite general power grid dynamics as adaptive dynamical networks, as introduced in Sec. IID, as long as the complex-frequency dynamics are well defined. In Sec. IIIB, we will perform this reformulation for the classical Kuramoto model with inertia. In Sec. IIIC, we derive an elegant equation entirely in terms of the matrix of complex couplings for the normal form, in which the network topology does not appear explicitly.

These reformulations generally come at the price of a larger phase space, which is typical for adaptive networks. In general, the phase space has  $4N + 4E$  dimensions, where  $N$  is the number of nodes and  $E$  is the number of edges in the power grid. The normal form is a notable exception to this rule, as demonstrated in Sec. IIIC, the phase space has a dimension of only  $4E$ . These additional degrees of freedom have already been shown to reveal new phenomena in power grids [21] and are useful for enabling analytical considerations. However, we do not expect them to enhance simulation performance.

### B. Adaptive Kuramoto model with inertia

The Kuramoto model with inertia is the classical model to describe a generator in a power grid [8]. It is used to describe the short-term behavior of the generator, also called the first swing. For this reason, it is also called the swing equation in this context. It is given by

$$\dot{\theta}_h = \omega_h, \quad (24)$$

$$\dot{\omega}_h = \frac{1}{2H_h}(P_h^s - D_h\omega_h - \sum_m P_{hm}), \quad (25)$$

where  $\theta_h$ ,  $\omega_h$ , and  $P_h^s$  are the phase angle, angular frequency, and active-power set point of node  $h$ .  $D_h$  is the damping coefficient and  $H_h$  is the inertia constant.

As the Kuramoto model with inertia has no voltage dynamics, the complex frequency is purely imaginary,  $\eta_h = j\omega_h$ . Using the relation between the coupling and the complex power [see Eq. (17)] and the coupling dynamics [see Eq. (21)], we can rewrite the Kuramoto model with inertia as the following adaptive network:

$$\dot{\eta}_h = \frac{1}{2H_h} \left( jP_h^s - D_h\eta_h - \frac{j}{2} \sum_m (K_{hm} + \bar{K}_{hm}) \right), \quad (26)$$

$$\dot{K}_{hm} = (\eta_h + \bar{\eta}_m)K_{hm}. \quad (27)$$

As the complex-coupling dynamics given above are formulated entirely in terms of invariants of the limit cycle, the phases do not appear explicitly. Thus synchronization at arbitrary frequencies is represented here by convergence to different fixed points, rather than limit cycles. For cluster synchronization, where several frequencies coexist, the clusters are internally approximately at fixed points, while the coupling between them oscillates rapidly. This formulation thus automatically realizes a fast-slow separation of variables for these common asymptotic states.

It is important to note that this form of adaptive power grid dynamics is not the same as the formulation introduced in Ref. [21]. The key difference between the two approaches is that the authors of Ref. [21] introduce a so-called pseudocoupling matrix in order to bring their specific system into the adaptive form. We, on the other hand, through the complex couplings introduced in Eq. (6), present a universal methodology to transform power grids into an adaptive form as long as the complex frequency for the nodal dynamics can be defined.

### C. Self-contained complex-coupling dynamics

By considering the equations of  $\eta$ , the normal form can be rewritten as an adaptive equation in a similar way to the Kuramoto model above. Instead, we can also directly combine the normal-form equations (see Sec. IIC) for  $\eta$  and the complex couplings  $K_{km}$ . These equations provide a self-contained dynamical system expressed entirely in terms of invariants of the limit cycle. For notational simplicity, we first neglect the internal variables  $x_h$ . Then, the entire power grid dynamics are given by

$$\dot{K}_{hm} = (\eta_h + \bar{\eta}_m)K_{hm},$$

$$\eta_h = g_h(P_h, Q_h, v_h),$$

$$P_h + jQ_h = \sum_m K_{hm}, \quad (28)$$

$$v_m = \frac{K_{mm}}{L_{mm}},$$

where  $P_h$ ,  $Q_h$ , and  $v_h$  are again the active and reactive power and the square of the voltage magnitude. Remarkably, this system of differential equations depends only

on the diagonal of the Laplacian  $L_{hm}$ , i.e., the weighted degrees. The line admittances are only encoded in the initial conditions.

If there are internal degrees of freedom  $x_h$  of the normal form, then there are dynamical variables at the node as well. Further, expressing  $g_h$  in terms of  $S = P + jQ$  and  $\bar{S} = P - jQ$  directly, we obtain the remarkable class of matrix dynamical systems:

$$\begin{aligned} \dot{K}_{hm} &= (\eta_h + \bar{\eta}_m)K_{hm}, \\ \eta_h &= g_h^v \left( \sum_m K_{hm}, \sum_m \bar{K}_{hm}, K_{hh}, x_h \right), \\ \dot{x}_h &= g_h^{x_c} \left( \sum_m K_{hm}, \sum_m \bar{K}_{hm}, K_{hh}, x_h \right). \end{aligned} \quad (29)$$

The normal form, which has been introduced in Ref. [10], is a promising model that can be used for technology-independent modeling of power grid components. However, the formulation presented in Ref. [10] so far has not enabled linear-stability analyses of entire networks. Expressing power networks via our elemental coupling dynamics provides many opportunities for future research, especially for stability analyses of the collective dynamics of future power grids. In the following, we employ the coupling terms to design complex-frequency dynamics that stabilize the power grid.

#### IV. GFI DESIGN AS A BILINEAR CONTROL PROBLEM

In Ref. [10], the normal form is introduced as a way to parametrize the space of plausible grid actors. This allows us to obtain a unified description of inverter designs and existing machines. However, it is important to also ask which points in this space would provide stable dynamical laws for the power grid.

We assume that we have a perfect voltage source that we can steer freely, an assumption that is typical in the study of grid-forming control [5,6]. Below, we will see that the complex-coupling variables allow us to cast this problem into the form of a bilinear-quadratic control problem. We also derive a quasilocal Lyapunov-function-based controller that is globally synchronizing.

##### A. Grid-forming control as a normal-form tracking problem

As noted above, the variables used in the normal form to express the coupling of the grid into the grid-forming actor are exactly those that a grid-forming actor seeks to control. We can assume that the grid-forming actor has (possibly time-dependent) set points  $v^s$ ,  $P^s$ , and  $Q^s$  for the desired active and reactive power and the square of the voltage amplitude. Then, we can write the normal form in terms

of the error coordinates  $e(t)$ , the difference between the desired and actual quantities. The control problem of grid-forming actors is thus reduced to a *tracking problem* with a feedback loop. The set points act as the reference  $r(t)$  that should be tracked and the complex frequency is the control input  $u(t)$  by which the power flow on the grid should be controlled. This is illustrated in Fig. 1. If we require the feedback loop to be a linear time-invariant system, we arrive exactly at the internally linearized normal-form equations already discussed in Ref. [10], which are valid near the desired state.

##### B. Complex voltage

Viewed in this way, the challenge of designing a good grid-forming control is a decentralized bilinear feedback control problem, as described in Sec. II E. If we use the complex voltages  $v(t)$  as the states  $y(t)$  and the complex frequency as the control input  $u(t)$ , the underlying bilinear system reads as

$$\dot{y}(t) = \sum_{a=1}^A \eta_a(t) F^a y(t), \quad (30)$$

where each system matrix  $F^a$  has only one entry. The rows and columns of  $F^a$  are the indices of the nodes in  $\mathcal{N}$ . The elements of  $F^a$  are given by

$$F_{hm}^a = \begin{cases} 1, & \text{if } a = k = m, \\ 0, & \text{otherwise,} \end{cases} \quad (31)$$

where  $h$  and  $m$  denote the nodes in  $\mathcal{N}$ . This system has the advantage that it is very simple and elegant and is directly formulated in physically meaningful variables. However, the observed power and voltage-amplitude mismatches that are required for the feedback are quadratic functions of the state variables and the asymptotic state that should be achieved is not a fixed point but a limit cycle. The complex-coupling formulation solves both of these issues.

##### C. Complex couplings

The power grid dynamics are fully described by the coupling terms  $K_{hm}$ . We consider only those lines  $l$  the admittances of which are nonzero, corresponding to the set of links  $\mathcal{L}$  (including self-loops) in the underlying power grid. We will treat  $K_{hm}$ ,  $\bar{K}_{hm}$ ,  $K_{mh}$ , and  $\bar{K}_{mh}$  as separate variables and the two directions of the edge between  $h$  and  $m \neq h$  as two distinct links  $l = (h, m) \neq (m, h) = l'$ . Thus the state vector  $y$  is given by

$$y(t) = (K_{l_1}, K_{l'_1}, \dots, K_{l_d}, K_{l'_d}, \bar{K}_{l_1}, \bar{K}_{l'_1}, \dots, \bar{K}_{l_d}, \bar{K}_{l'_d})^T. \quad (32)$$

The nodal complex frequencies  $u(t) = (\eta_1, \bar{\eta}_1, \dots, \eta_n, \bar{\eta}_n)^T$  act as the control input into the system.

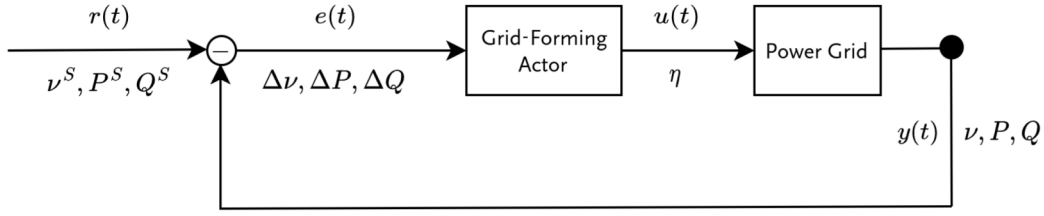


FIG. 1. A block diagram that represents a single grid-forming actor coupled to the power grid. The GFI prescribes a control input  $u$ , the complex frequency, to the power grid, which then leads to an observed output  $y(t)$ , the power flow and voltage, which is used as control feedback by the normal form.

We define the system matrices  $R_a$  and  $\tilde{R}_a$  to bring the system into a bilinear form, as defined in Eq. (14). We have two controls per node  $h$ :  $\eta_h$  and  $\bar{\eta}_h$ . The system matrices can be decomposed into the following blocks:

$$R_a = \left( \begin{array}{c|c} O^a & 0 \\ \hline 0 & T^a \end{array} \right), \quad (33)$$

$$\tilde{R}_a = \left( \begin{array}{c|c} T^a & 0 \\ \hline 0 & O^a \end{array} \right). \quad (34)$$

We introduce the shorthand notation  $o(l)$  and  $t(l)$  for the origin and target of a link:

$$l = (o(l), t(l)). \quad (35)$$

Then, the origin matrix  $O^a$  projects onto those links the origin of which is  $a$  i.e.,  $o(e) = a$ . The rows and column indices of  $O^a$  correspond to links of the graph and we can explicitly write

$$O_{ll'}^a = \begin{cases} 1, & \text{if } l = l' \text{ and } o(l) = a, \\ 0, & \text{otherwise,} \end{cases} \quad (36)$$

where  $l$  and  $l'$  are the links in  $\mathcal{L}$ .

The target matrix  $T^a$  projects onto those links the target of which is  $h$ :

$$T_{ll'}^a = \begin{cases} 1, & \text{if } l = l' \text{ and } t(l) = a, \\ 0, & \text{otherwise.} \end{cases} \quad (37)$$

With these matrices, we have the following bilinear form of the control problem:

$$\dot{y}(t) = \sum_{h \in \mathcal{N}} \eta_a R_a y(t) + \bar{\eta}_a \tilde{R}_a y(t). \quad (38)$$

Taking these equations as the underlying system to be controlled by the complex frequency means that the tracking errors are now just linear combinations of the system state and the reference signal. Thus, we have cast the challenge of finding stabilizing grid-forming controllers for the

power grid in terms of a decentralized linear-feedback-control synthesis of a bilinear-tracking-control problem [see Eq. (14)].

We should note that this formulation is not without challenges. The fact that we have one coupling per edge, while we have one voltage per node, implies that the complex frequency cannot achieve arbitrary couplings from any starting position. Our linear state space decomposes into reachable layers. As we will see further below, this complicates the synthesis of elegant dynamical laws in this formulation.

Furthermore, we want to note that the dynamics for the power flow in Eq. (C7) and the square of the voltage in Eq. (C8) have a self-contained bilinear structure as well. The derivation can be found in Appendix C 1.

#### D. A quasilocal, error-minimizing, and globally synchronizing grid control

So far, we have formulated a bilinear tracking control problem with linear feedback. The next problem to solve is to design a controller that effectively stabilizes the system. It is natural to consider a quadratic cost function  $V$  in the error coordinates of the normal form:

$$\begin{aligned} V(S, \bar{S}, v) &= \sum_h |S_h - S_h^s|^2 + (v_h - v_h^s)^2 \\ &= \sum_h |\Delta S_h|^2 + (\Delta v_h)^2 \geq 0, \end{aligned} \quad (39)$$

where  $S_h$  is the nodal apparent power and  $v_h$  is the square of the voltage magnitude at node  $h$ .

This cost function can serve as a control-Lyapunov function (CLF) for our system. CLFs are an extension of the Lyapunov function from general dynamical systems to systems with control inputs  $u$  [32]. According to Artstein's theorem [33], if a CLF for a system exists, then the system is asymptotically stabilizable, meaning that for any state  $y$ , a control  $u(y)$  can be constructed that asymptotically guides the system back to a fixed point.

Recall that a control-affine system, as described in Sec. II E, is given by

$$\dot{y} = \mathbf{F}(y) + \mathbf{G}(y)\mathbf{u}. \quad (13)$$

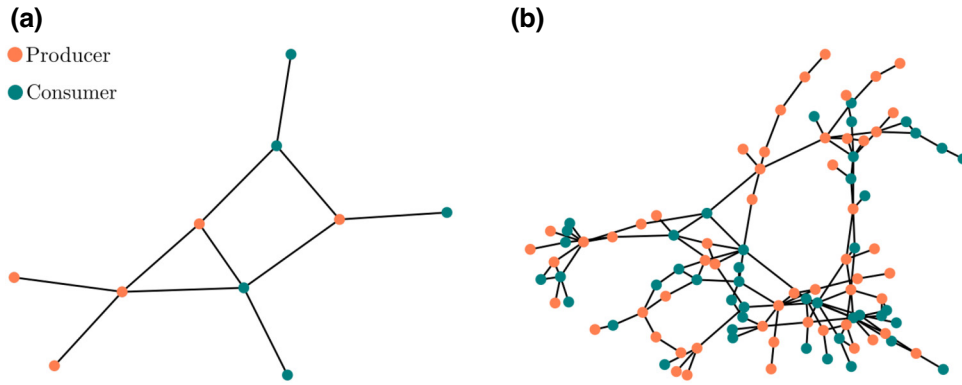


FIG. 2. The typologies of the (a) ten-node and (b) 100 node test power grids. Net producers are shown in orange and net consumers are shown in green.

For such systems, a stabilizing control can be explicitly constructed from any suitable  $V$  for which the gradient  $\dot{V}$  does not vanish except at the fixed point. The most well-known formula for constructing a stabilizing controller is given by Sontag's formula [33]. However, in our context, we have  $\mathbf{F}(\mathbf{y}) = 0$  and a stabilizing control is already given by

$$u^c = -(\nabla V \mathbf{G}(\mathbf{y}))^T, \quad (40)$$

where  $u^c$  is the control input, leading to the dynamics  $\dot{V} = -u^c \dot{u}^c$ .

Using the square norm of the error coordinates of the tracking problem, given in Eq. (39), in this formula leads to the quasilocal control law:

$$-\delta \eta_h^c := \Delta S_h \bar{S}_h + 2\Delta v_h v_h + \sum_m K_{mh} \Delta \bar{S}_m. \quad (41)$$

The full derivation of this control law, as well as a more in-depth introduction to CLF, can be found in Appendix D. While we are controlling derivatives via the complex frequency, the voltage itself is nevertheless explicitly accounted for through the CLF presented in Eq. (39).

The control law in Eq. (40) has the property that

$$\dot{V} = -\sum_h \delta \bar{\eta}_h^c \delta \eta_h^c \leq 0. \quad (42)$$

Thus, the mismatch between the realized grid state and the desired grid state cannot grow under this dynamical law. As the cost function is positive definite and vanishes at the desired grid state, we immediately obtain that this control law also stabilizes the operating state of the system. However, we cannot conclude that the system will always find the global minimum of the cost function. While the cost function is quadratic and thus convex on the full space of couplings, its projection on the reachable layers is not. Therefore, we have to contend with local minima of the cost function. However, these local minima are still globally synchronized, because they still imply that  $\dot{V}$  and thus  $\delta \eta$  go to zero. We show in Appendix D 2 that the local minima of  $V$ , subject to the constraint that the  $h$  arise from some  $v$ , exactly require  $\eta_h^c = 0$ .

It is also noteworthy that this control law seems to stabilize fair power sharing at the global minimum of the cost function, without coupling the power imbalance to the

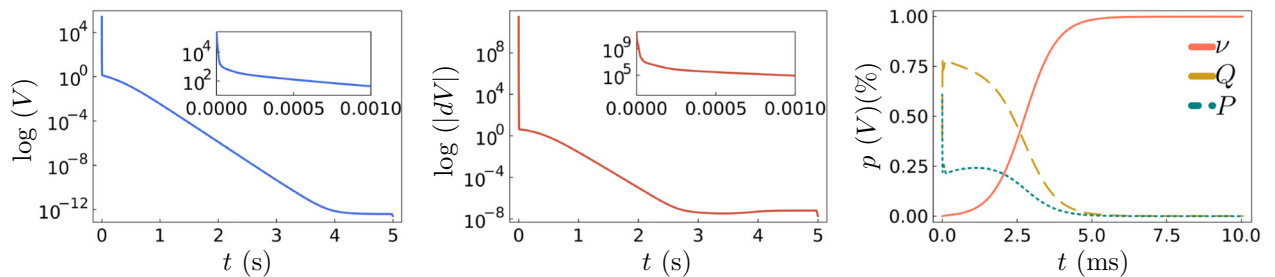


FIG. 3. The CLF  $V$  and its derivative  $dV$  after a voltage perturbation to a node. It can be seen that the CLF reduces rapidly in the first milliseconds by compensating the active- and reactive-power errors that can be seen in the right-hand figure, which shows the relative shares of the CLF to its three components,  $\Delta P$ ,  $\Delta Q$ , and  $\Delta v$ . After the initial drop, the CLF decreases further and then saturates after approximately 4 s.

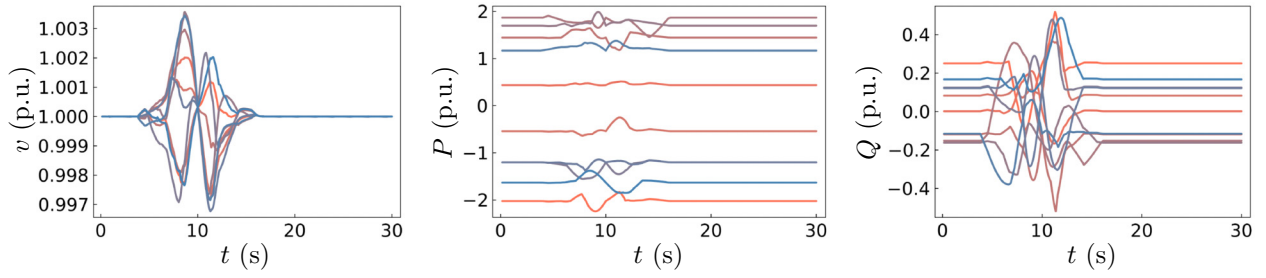


FIG. 4. The voltage magnitude and the active- and reactive-power transients during the set-point fluctuations of the ten-node test system.

frequency (see Sec. IV D 1). The system always synchronizes exactly at the design frequency.

All points that satisfy the power-flow equations have  $V = 0$  and thus are stable. This is in direct contrast to the requirements typically imposed on the power-flow solution for guaranteeing stability. For example, Ref. [15] requires that the difference between the phase angles between voltages is small and, in particular, not larger than  $\pi/2$ . Thus  $v_i \bar{v}_j$  has to have a positive real part. The stability of the Kuramoto model is likewise only guaranteed if the effective network Laplacian, weighted with the cosine of the phase angle differences, is positive definite [7]. This follows easily from the condition that the differences are smaller than  $\pi/2$  if the system is lossless. However, the condition is complicated in general.

The disadvantage of this controller is that it is not decentralized but only quasilocal, as  $\eta_h^c$  requires information about the state of the lines and nodes adjacent to  $h$ . Thus, the resulting controller is not in the space of behaviors parametrized by the normal form [10]. It is, however, similar in its communication needs to distributed averaging controllers proposed to tackle secondary control objectives in power grids [34,35].

It should also be noted that this controller minimizes the cost function but is not an optimal control in the sense that it minimizes the integral of the cost over time.

We consider this controller and the intriguing dynamics it provides as a proof of concept that the formulations given here are highly promising for further analytical investigation.

It will be especially worthwhile to investigate how to incorporate a decentrality constraint. Furthermore, it has to be noted that the controller depends highly on the choice of the cost function to use as CLF. Hence, it is valuable to find and analyze other possible CLFs and their corresponding controllers. This is beyond the scope of this work and will be addressed in subsequent papers.

### 1. Examples

We generate a ten-bus synthetic power grid to validate the control law in a simulation example. To create the test power grid, we adopt the synthetic power grid framework recently presented by the authors of Ref. [36]. In the interest of self-containment, we provide a concise overview of the key features of this algorithm and the simulation methods in Appendix D 1 a. Figure 2(a) shows the topology of the resulting synthetic grid.

We implement the complex frequency  $\eta^c$  given by the control law in Eq. (41) for the nodal dynamics of the synthetic grid. We calculate the voltage transients according to Eq. (7) and then define the currents and powers using Ohm’s law and Kirchhoff’s law. The software and data that

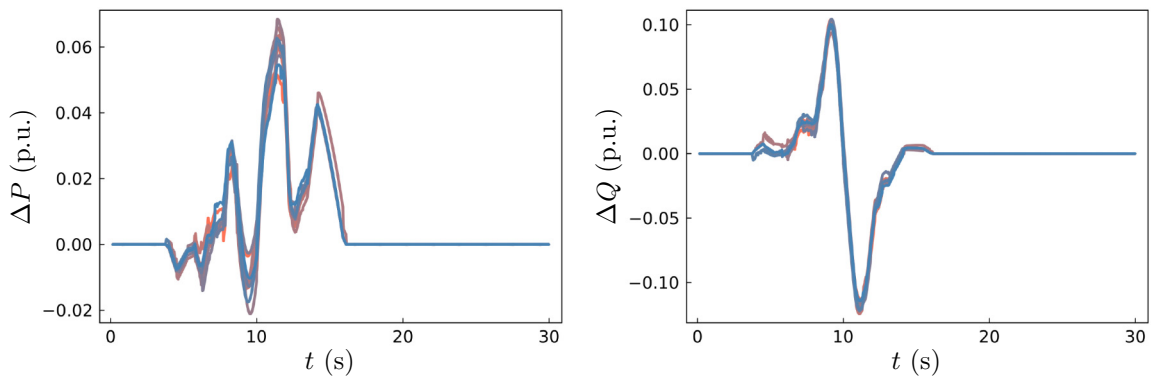


FIG. 5. The errors of the active- and reactive-power transients during the set-point fluctuations of the ten-node test system.

supports the findings of this study are openly available on Zenodo [37].

As an example, we decrease the voltage at a bus to 0.5 [per unit (p.u.)] and study the CLF  $V$  and its derivative  $dV$  as shown in Fig. 3. We can see that the CLF is rapidly decreasing in the first milliseconds of the simulation. Furthermore, we also analyze which of the error coordinates,  $\Delta P$ ,  $\Delta Q$ , and  $\Delta v$ , gives the largest share to the CLF. From the relative shares, we find that this rapid decrease is due to the reduction of the error in the active and reactive power. After this first initial drop, the CLF decreases further, which corresponds to the reduction in the voltage-magnitude errors. Then, the CLF saturates at  $10^{-17}$  after approximately 4 s, as also reflected by its derivative, which reaches  $10^{-8}$  after approximately 3 s.

Additionally, we use the control law for a proper tracking problem. In this example, we simulate a random superposition of sinusoidal fluctuations of the active-power set points at all nodes. Each fluctuation has a different period and amplitude and runs for one respective period. As these are drawn independently, the resulting set points are inconsistent during the fluctuation.

Note that due to the nonzero derivatives of the set points, we do not have the condition that  $\dot{V} < 0$ . As soon as the variation of the set points stops,  $V$  has to decrease. Nevertheless, the dynamics are constantly working to minimize the cost function and successfully track the desired set points.

Figure 4 provides the transients of the voltage magnitude and the active and reactive power. We find that the active and reactive powers are adjusted to the new set points. The system does not become unstable, although the set points are highly unbalanced during the transient period. Remarkably, the voltage magnitudes stay very close to their nominal values, although the system is under severe stress. This is a further success of the designed control law. Figure 5 shows the errors of the rated power and the set points. As the active-power set points are highly unbalanced during the fluctuations, it is impossible for the system to follow the set points perfectly. Instead, our control law adjusts the power outputs such that all nodes share the mismatch, which is also referred to as equal sharing. After all fluctuations have vanished, the control law smoothly brings the system back into the previously synchronized and stable state.

Further examples, such as the so-called black-start capabilities and simulations for larger networks, can be found in Appendix D 1.

## V. CONCLUSIONS

The stability of future power grids, particularly in the context of the wide-scale integration of renewable energy

sources via power-electronic inverters, remains a challenging topic. While there have been numerous stability analyses of power-electronic inverters connected to an infinite bus bar [5,17], and stability analyses of networks consisting purely of conventional generation [7,9], the stability of inverter-dominated networks is not well understood and is an area of active research.

To address these challenges, the normal form [10], a dynamic technology-neutral model for grid-forming actors, has recently been introduced. The normal form can describe the dynamics of all grid-forming actors, including grid-forming inverters and conventional synchronous generators, and can thus capture the transitional periods when a reduced number of synchronous generators are still connected to the grid, as well as future highly heterogeneous inverter-dominated systems.

In this paper, we have shown that the concept of the complex frequency [11], combined with the newly introduced dynamic complex couplings defined in Eq. (21), allows for an elegant adaptive network formulation of the Kuramoto model with inertia. When combined with the normal-form description of grid-forming actors, we obtain self-contained matrix dynamics for general power grid dynamics in which the grid topology does not appear explicitly. Beyond what we have shown here, the complex-coupling dynamics allow for rewriting a large class of dynamical equations as adaptive.

As considerable progress has been made recently in understanding the properties of adaptive networks [19,20], this opens up a new avenue for understanding power grids beyond the currently used generator models. We expect that our formulations will be useful in deriving widely applicable analytical stability results in the future.

Furthermore, we have seen that the design of stable grid-forming actors can be cast as a bilinear control problem. The control problem simplifies due to the control-affine nature of the bilinear system and allows us to define a stabilizing control input. By defining a suitable CLF, a control law has been derived that leads to global synchronization. However, it should be noted that the resulting controller is not completely decentralized, as it requires information from adjacent nodes. Thus it resembles distributed averaging control [34], which is usually considered for secondary control objectives.

The formulation of power grids using the combination of the complex frequency and the normal form shows surprising elegance. This paper has mapped out some, though by no means all, of the relevant results from control theory, electrical engineering, and statistical physics to demonstrate that there is considerable synergy in this approach. Excitingly, the methods include the full physics of balanced three-phase power grids, including losses and generic voltage dynamics. These are known to be important to obtain a full understanding of the

collective dynamics of the system [9,23]. The proposed models and formulations thus offer a pathway for further research and development in this area, to ensure the stability and reliability of future renewable energy systems.

### ACKNOWLEDGMENTS

We would like to thank Jakob Niehues and Jürgen Kurths for their discussions and detailed comments on the manuscript. The work was supported in part by the German Research Foundation (Deutsche Forschungsgemeinschaft, DFG) under Grant No. KU 837/39-2 and the Federal Ministry for Economic Affairs and Climate Action (Bundesministerium für Wirtschaft und Klimaschutz, BMWK) under Grant No. 03EI1016A. A.B. acknowledges support from the German Academic Scholarship Foundation.

### APPENDIX

In Appendix A, we collect useful information on complex variables for working with the formulation introduced in the main text. Appendix B gives a minor extension of the formulation above to the case of dynamical lines with a homogeneous ratio of resistance to inductance. Appendix D gives further information on the new control law presented in the main text, including a more detailed derivation and the characterization of the local minima of the CLF.

#### APPENDIX A: COMPLEX VARIABLES

The formulation of the power grid in terms of complex variables is succinct but requires that some care is taken, especially when working with derivatives of the functions involved. This is due to the fact that complex conjugation of a complex number  $z$  is not a complex differentiable function. We can work around this fact by treating  $\bar{z}$  as a separate variable. To illustrate how this arises, we will start from a real-valued system and derive the correct equations. For this appendix, we will call the complex conjugate of a variable  $z^*$  to differentiate it more clearly from  $\bar{z}$ .

Consider a dynamical system with two  $d$ -dimensional vectors  $x$  and  $y$ :

$$\dot{x} = f^x(x, y), \quad (\text{A1})$$

$$\dot{y} = f^y(x, y). \quad (\text{A2})$$

We can write  $z = x + jy$ . Then, we can write the dynamics as

$$\dot{z} = f^z(z), \quad (\text{A3})$$

$$:= f^x(\Re(z), \Im(z)) + jf^y(\Re(z), \Im(z)). \quad (\text{A4})$$

Unless  $f^x$  and  $f^y$  satisfy the Cauchy-Riemann equation,  $f^z(z)$  is not differentiable in the complex sense as a function of  $z$ , even if  $f^x$  and  $f^y$  are real differentiable. In particular,  $\Re(z)$  is not a differentiable function of  $z$ .

However, if we introduce two new variables as “complex linear combinations”  $z = x + jy$  and  $\bar{z} = x - jy$ , we can write  $x = \frac{1}{2}(z + \bar{z})$ , which is separately differentiable in  $z$  and  $\bar{z}$ . To take this derivative, we treat  $z$  and  $\bar{z}$  as independent complex variables. Taking this seriously means that  $x$  and  $y$  can now be complex. If we evaluate the system on  $\bar{z} = z^*$ , i.e., we enforce by hand that  $\bar{z}$  really is the complex conjugate,  $x$  will be real.

We can then cast the system as follows:

$$\dot{z} = f^{hol}(z, \bar{z}) \quad (\text{A5})$$

$$:= f^x\left(\frac{1}{2}(z + \bar{z}), \frac{1}{2j}(z - \bar{z})\right) + jf^y\left(\frac{1}{2}(z + \bar{z}), \frac{1}{2j}(z - \bar{z})\right), \quad (\text{A6})$$

$$\dot{\bar{z}} = \bar{f}^{hol}(z, \bar{z}) \quad (\text{A7})$$

$$:= f^x\left(\frac{1}{2}(z + \bar{z}), \frac{1}{2j}(z - \bar{z})\right) - jf^y\left(\frac{1}{2}(z + \bar{z}), \frac{1}{2j}(z - \bar{z})\right). \quad (\text{A8})$$

Now,  $f^{hol}$  and  $\bar{f}^{hol}$  have a good chance of being differentiable as functions of  $z$  and  $\bar{z}$ . In particular, this will be the case whenever we can analytically extend  $f^x$  and  $f^y$  into the complex plane. For example, this will work for polynomials.

#### 1. Wirtinger derivatives

While extending the function to the complex plane might not always be possible, we can still access the “derivative in the  $z, \bar{z}$  direction” without actually extending the underlying real functions. Writing  $\partial_x$  for  $\partial/\partial x$ , then, for the complexified function, we have the following:

$$\partial_z f^{hol}(z, \bar{z}) = \frac{1}{2}(\partial_x - j\partial_y)(f^x + jf^y), \quad (\text{A9})$$

$$\partial_{\bar{z}} f^{hol}(z, \bar{z}) = \frac{1}{2}(\partial_x + j\partial_y)(f^x + jf^y), \quad (\text{A10})$$

$$\partial_z \bar{f}^{hol}(z, \bar{z}) = \frac{1}{2}(\partial_x - j\partial_y)(f^x - jf^y), \quad (\text{A11})$$

$$\partial_{\bar{z}} \bar{f}^{hol}(z, \bar{z}) = \frac{1}{2}(\partial_x + j\partial_y)(f^x - jf^y). \quad (\text{A12})$$

The right-hand side is well defined without complexification. It can be evaluated using only the real functions  $f^x$  and  $f^y$  and their derivatives. The derivative operator  $\partial_{z/\bar{z}} = \partial_x \mp j\partial_y$  applied to a complex-valued function on

the real domain of  $x$  and  $y$  is called the Wirtinger derivative. Note that the Cauchy-Riemann equation is simply  $\partial_{\bar{z}}f = 0$ .

Note that we have

$$\partial_z z = 1, \quad (\text{A13})$$

$$\partial_{\bar{z}} z = 0, \quad (\text{A14})$$

$$\partial_z \bar{z} = 0, \quad (\text{A15})$$

$$\partial_{\bar{z}} \bar{z} = 1, \quad (\text{A16})$$

as might be expected.

## 2. Extrema with Wirtinger derivatives

To illustrate the use of these equations, consider the optimization of a real function  $V(x, y)$ . The first-order condition for extrema is

$$\partial_x V = 0, \quad (\text{A17})$$

$$\partial_y V = 0. \quad (\text{A18})$$

If we write the function in terms of  $V(z, \bar{z})$ , we can write this condition as

$$\partial_z V = 0, \quad (\text{A19})$$

$$\partial_{\bar{z}} V = 0. \quad (\text{A20})$$

For example, take  $V = xy + x^2 + y^2$ ; then,  $V = z\bar{z} + (1/4j)(z + \bar{z})(z - \bar{z})$ . The complex derivative conditions then give

$$\partial_z V = \bar{z} + \frac{1}{4j}(z - \bar{z} + z + \bar{z}), \quad (\text{A21})$$

$$0 = \bar{z} + \frac{1}{2j}z, \quad (\text{A22})$$

$$\partial_{\bar{z}} V = z + \frac{1}{4j}(z - \bar{z} - z - \bar{z}), \quad (\text{A23})$$

$$0 = z - \frac{1}{2j}\bar{z}, \quad (\text{A24})$$

which can readily be solved by inserting the second equation into the first. Note that the second equation can be obtained from complex conjugating the first, which can also be verified directly from the definition of the Wirtinger derivatives applied to a real function. Depending on the functions at hand, it can be considerably simpler or harder to work in complex coordinates.

## APPENDIX B: LINE DYNAMICS

The main text of this paper is concerned with the dynamics of power systems and power lines in the quasi-steady-state approximation, i.e., the current on the lines is given

by Eq. (18):

$$i_{hm}^{qss} = Y_{hm}(v_h - v_m). \quad (\text{B1})$$

In reality, a change in voltage at one end of the line does not lead to an instantaneous change in current at the other. A dynamical model for lines that takes this into account better is the  $RL$ -line model. This describes lines as a series circuit of an inductance and a resistor  $R$ . The inductance is typically called  $L$ . To avoid confusion with the Laplacian matrix, we call it  $\Lambda$ . With complex voltage and current and in a frame rotating with  $\Omega$ , this leads to the differential equation

$$\Lambda_{hm} \frac{di_{hm}}{dt} = v_h - v_m - R_{hm}i_{hm} - j\Omega\Lambda_{hm}i_{hm}. \quad (\text{B2})$$

Introducing the complex impedance  $Z_{hm} = R_{hm} - j\Omega\Lambda_{hm}$ , which is the reciprocal of the admittance  $Y_{hm}$  we can write this as

$$\Lambda_{hm} \frac{di_{hm}}{dt} = v_h - v_m - Z_{hm}i_{hm}, \quad (\text{B3})$$

$$\Lambda_{hm} \frac{di_{hm}}{dt} = Z_{hm}(Y_{hm}(v_h - v_m) - i_{hm}), \quad (\text{B4})$$

$$\frac{di_{hm}}{dt} = \frac{Z_{hm}}{\Lambda_{hm}}(i_{hm}^{qss} - i_{hm}), \quad (\text{B5})$$

$$\frac{di_{hm}}{dt} = \left( \frac{R_{hm}}{\Lambda_{hm}} + j\Omega \right) (i_{hm}^{qss} - i_{hm}). \quad (\text{B6})$$

For the power on the line, we immediately obtain

$$\frac{dS_{hm}}{dt} = \eta_h S_{hm} + \left( \frac{R_{hm}}{\Lambda_{hm}} - j\Omega \right) (S_{hm}^{qss} - S_{hm}) \quad (\text{B7})$$

and  $S_{hm}^{qss}$  follows the equation of Sec. D 1.

A remarkable simplification arises if  $R_{hm}/\Lambda_{hm}$  is assumed to be homogeneous throughout the network. This is plausible, as both  $R$  and  $\Lambda$  are proportional to the length of the line. Call their ratio  $\alpha_{rl} = R/\Lambda$ ; then, the dynamics of the power can be given in terms of the  $K_{hm}$  directly:

$$\dot{S}_h = \eta_h S_h + (\alpha_{rl} - j\Omega) (S_h^{qss} - S_h), \quad (\text{B8})$$

$$\dot{S}_h = \eta_h S_h + (\alpha_{rl} - j\Omega) \left( \sum_m K_{hm} - S_h \right). \quad (\text{B9})$$

Thus, this model of dynamic lines leads to the same adaptive-coupling formulation in terms of  $K_{hm}$ , the only difference being that the nodal dynamics get augmented by what is essentially a low-pass filter for the part of the nodal power variation that arises due to the coupling.

### APPENDIX C: POWER-FLOW VARIABLES

The complex power flow  $S_{hm}$  on a line connecting node  $h$  and  $m$  is defined as follows:

$$i_{hm} = Y_{hm}(v_h - v_m), \quad (C1)$$

$$S_{hm} = v_h \bar{i}_{hm} = \bar{Y}_{hm} v_h - \bar{Y}_{hm} v_h \bar{v}_m. \quad (C2)$$

The dynamics for the power flow then leads to

$$\dot{S}_{hm} = \dot{v}_h \bar{Y}_{hm} \bar{v}_h + v_h \bar{Y}_{hm} \dot{\bar{v}}_h - \dot{v}_h \bar{Y}_{hm} \bar{v}_m - v_h \bar{Y}_{hm} \dot{\bar{v}}_m \quad (C3)$$

$$= \eta_h \bar{Y}_{hm} v_h + \bar{\eta}_h v_h \bar{Y}_{hm} - v_h \eta_h \bar{Y}_{hm} \bar{v}_m - v_h \bar{Y}_{hm} \bar{v}_m \bar{\eta}_m \quad (C4)$$

$$= S_{hm} \eta_h + v_h \bar{Y}_{hm} \bar{\eta}_h - v_h \bar{Y}_{hm} \bar{v}_m \bar{\eta}_m \quad (C5)$$

$$= S_{hm} \eta_h + v_h \bar{Y}_{hm} \bar{\eta}_h + S_{hm} \bar{\eta}_m - v_h \bar{Y}_{hm} \bar{\eta}_m \quad (C6)$$

$$= S_{hm} (\eta_h + \bar{\eta}_m) + v_h \bar{Y}_{hm} (\bar{\eta}_h - \bar{\eta}_m). \quad (C7)$$

If we augment these with the dynamics for the square of the voltage,  $v_h = v_h \bar{v}_h$ ,

$$\dot{v}_h = v_h (\eta_h + \bar{\eta}_h). \quad (C8)$$

This again provides a self-contained set of equations for the power flow and the voltage amplitude as a function of the complex frequency at the nodes.

#### 1. Power-flow bilinear structure

For the power-flow dynamics, the state vector  $y$  is given by

$$y(t) = (v_1, \dots, v_n, S_{l_1}, S_{l'_1}, \dots, S_{l_d}, S_{l'_d}, \bar{S}_{l_1}, \bar{S}_{l'_1}, \dots, \bar{S}_{l_d}, \bar{S}_{l'_d})^T. \quad (C9)$$

$S_l = S_{mh}$  denotes the power flow on the link  $l$  as seen from  $t(l) = m$  and  $S_{l'}$  denotes the flow in the opposite direction, as seen from  $h$ .

To bring the system into a bilinear form, we have to define system matrices. We have two controls per node,  $h$ ,  $\eta_h$ ,  $\bar{\eta}_h$ , and we denote the corresponding system matrices as  $N_a$  and  $\tilde{N}_a$ , respectively. The matrices can then be decomposed into the following block-matrix form:

$$N_a = \left( \begin{array}{c|c|c} F^a & 0 & 0 \\ \hline 0 & O^a & 0 \\ \hline M^a & 0 & T^a \end{array} \right), \quad (C10)$$

$$\tilde{N}_a = \left( \begin{array}{c|c|c} F^a & 0 & 0 \\ \hline M^{*a} & T^a & 0 \\ \hline 0 & 0 & O^a \end{array} \right), \quad (C11)$$

where the blocks  $F^a$ ,  $O^a$ , and  $T^a$  have been defined in Secs. IV B–III A.  $M^a$  is a mixed block handling the interaction

between the voltages at the nodes and the power flow on the links and incorporates the line admittances.

The column indices of  $M^a$  are links and the row indices are vertices. The elements of the mixed block are defined as

$$M_{lh}^a = \begin{cases} Y_l, & \text{if } k = a = o(l), \\ -Y_l, & \text{if } l = (h, a), \\ 0, & \text{otherwise.} \end{cases} \quad (C12)$$

The block  $\bar{M}_a$  is the element-wise complex conjugate of  $M_a$ .

### APPENDIX D: CONTROL-LYAPUNOV FUNCTION

A function  $V(y)$  is a CLF for a controlled dynamical system  $\dot{y} = f(y, u)$  and the origin 0, if (i) it is continuously differentiable and (ii) it is positive definite, meaning that  $V(y) > 0$  for all  $y \neq 0$  and  $V(0) = 0$ . For all  $y \neq 0$ , there exists a  $u$  such that

$$\dot{V} < 0 \quad (D1)$$

and there exists a  $u^*$  such that  $\dot{V}(0, u^*) = 0$ .

CLFs are particularly useful for control-affine systems:

$$\dot{y} = \mathbf{F}(y) + \mathbf{G}(y)\mathbf{u}. \quad (D2)$$

The derivative of a potential CLF  $V$  for such a system is given by

$$\dot{V} = \frac{\partial V^T}{\partial y} = \frac{\partial V^T}{\partial y} \mathbf{f}(y) + \frac{\partial V^T}{\partial y} \mathbf{G}(y)\mathbf{u} = \mathbf{a}(y) + \mathbf{b}(y)^T \mathbf{u}. \quad (D3)$$

As in our case  $a(y) = 0$ , a stabilizing controller is simply given by

$$\mathbf{u}^c = -\mathbf{b} \quad (D4)$$

which then results in the following derivative for  $V$ :

$$\dot{V} = -\mathbf{b}^2 \leq 0 \quad (D5)$$

and thus shows that  $V$  is a CLF up to the condition that  $\dot{V}$  must not become zero away from the origin.

We present the following CLF  $V$  for our system:

$$V(S, \bar{S}, v) = \sum_h |S_h - S_h^d|^2 + (v_h - v_h^d)^2 \geq 0 \quad (\text{D5})$$

$$= \sum_h \Delta S_h \Delta \bar{S}_h + \Delta v_h \Delta v_h. \quad (\text{D6})$$

Using Eqs. (20) and (C8) to get the derivatives of  $S_h$  and  $v_h$ , respectively, we obtain the following expression for  $\dot{V}$ :

$$\dot{V}(S, \bar{S}, v) = \sum_h \dot{S}_h \Delta \bar{S}_h + \Delta S_h \dot{\bar{S}}_h + 2\dot{v}_h \Delta v_h \quad (\text{D7})$$

$$= \sum_h S_h \eta_h \Delta \bar{S}_h + \Delta \bar{S}_h \sum_m K_{hm} \bar{\eta}_m + \Delta S_h \bar{\eta}_h \bar{S}_h + \Delta S_h \sum_m \bar{K}_{hm} \eta_m + 2\Delta v_h v_h (\eta_h + \bar{\eta}_h). \quad (\text{D8})$$

We rearrange the equation to isolate the control inputs  $\eta_h$  and  $\bar{\eta}_h$ :

$$\dot{V} = \sum_h \eta_h (S_h \Delta \bar{S}_h + 2\Delta v_h v_h) + \bar{\eta}_h (\Delta S_h \bar{\eta}_h \bar{S}_h + 2\Delta v_h v_h) + \sum_h \sum_m K_{hm} \bar{\eta}_m \Delta \bar{S}_h + \Delta S_h \bar{K}_{hm} \eta_m. \quad (\text{D9})$$

After switching the indices  $m$  and  $h$  in the second sum, we obtain  $\dot{V}$  in the form of Eq. (D2), which allows us to directly define the control:

$$\dot{V} = \sum_h \eta_h (S_h \Delta \bar{S}_h + 2\Delta v_h v_h + \sum_m \Delta S_m \bar{K}_{mh}) + \bar{\eta}_h (\Delta S_h \bar{S}_h + 2\Delta v_h v_h + \sum_m K_{mh} \Delta \bar{S}_m) \quad (\text{D10})$$

$$= \sum_h \eta_h \bar{b}_h + \bar{\eta}_h b_h, \quad (\text{D11})$$

$$b_h = \Delta S_h \bar{S}_h + 2\Delta v_h v_h + \sum_m K_{mh} \Delta \bar{S}_m. \quad (\text{D12})$$

Using the control law in Eq. (D3), we define the control for  $\eta^c$  as

$$\eta_h = \eta_h^c := -b_h = \Delta S_h \bar{S}_h + 2\Delta v_h v_h + \sum_m K_{mh} \Delta \bar{S}_m. \quad (\text{D13})$$

Then,  $\dot{V}$  is given by

$$\dot{V} = -2 \sum_h \bar{\eta}_h^c \eta_h^c \leq 0, \quad (\text{D14})$$

which shows that  $V$  is a CLF and  $\eta^c$  results in global asymptotic stability. For both the power flow and the

coupling dynamics, the state space is larger than the space of physically realizable flows. There is no requirement that a voltage  $v_h$  exists that can realize the  $K_{hm}$  given. However, if we start on the physical manifold, then by construction the dynamics driven by the complex frequency will stay on that manifold. The calculation showing this can be found in Sec. E 2.

## 1. Lyapunov-control-function examples

### a. Test systems

To create test power grids, we adopt the synthetic power grid framework recently presented by the authors of Ref. [36]. In the interest of self-containment, we provide a concise overview of the key features of this algorithm, adhering to the default structure outlined in Ref. [36].

All computations are conducted within a p.u. system. Utilizing the same p.u. system as detailed in Ref. [36], we set  $V_{\text{base}} = 380$  kV and  $P_{\text{base}} = 100$  MW as the reference voltage and power, respectively.

The power grid structures are generated through the random growth algorithm introduced in Ref. [38]. Line admittances and shunt admittances are computed based on standard line parameters for transmission systems operating at 380 kV, as specified by the German Energy Agency (dena) [39].

To simulate a realistic distribution of active-power demand and supply, we employ the ELMOD-DE data set [40], a dispatch model for the German Extra High Voltage (EHV) transmission system. The nodal dynamics of the system are given by the control law in Eq. (41).

For validation purposes, ensuring that the stability characteristics of the generated power grids mirror those of real systems, we employ a rejection-sampling approach. Prior to in-depth analysis, a small signal stability analysis [41] is conducted to ensure linear stability of the grids. Additionally, validation checks are performed to confirm that no lines in the grid experience overloads during normal operation.

For the simulation of the dynamical system, we use the DifferentialEquations.jl package [42] and the JULIA language [43]. We have used the RODAS4 solver with an absolute and relative tolerance of  $10^{-7}$ .

### b. Black start

To study a more severe control task, we also consider a black start of the ten-bus system, which means that we decrease all voltages to 0.01[p.u.]. We use this voltage magnitude as a voltage of 0.0[p.u.] is a fixed point of the dynamical system as discussed in Sec. III A. From Fig. 6, we can see that our control can perform a black start for the test system in 35 s.

However, the black-start capabilities are not given for arbitrary systems. Figure 7 shows an attempted black start of a 100-node system generated by the algorithm given in

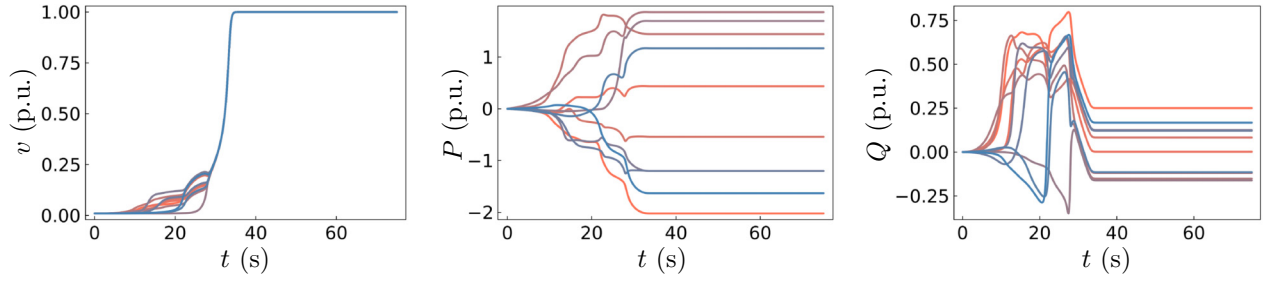


FIG. 6. The voltage magnitude and the active- and reactive-power transients during the black start of the ten-node test system.

Ref. [36]. It can be seen that the system voltages are not returning to their nominal values. The test system returns to another fixed point that is not the operating point of the grid.

## 2. Existence of the voltage

For both the power flow and the coupling dynamics, the state space is larger than the space of physically realizable flows. There is no requirement that a  $v_h$  exists that can realize the  $K_{hm}$  given. However, if we start on the physical manifold, then by construction, the dynamics driven by the complex frequency will stay on that manifold. We consider the local minima of  $V$  on the physical manifold:

$$\min_{S, \bar{S}, v, \lambda^S, \bar{\lambda}^S, \lambda^v, v, \bar{v}} \left( V(S, \bar{S}, v) - \bar{\lambda}^S \cdot (S - [v]\bar{Y}\bar{v}) - \lambda^S \cdot (S - [\bar{v}]Yv) - \lambda^v \cdot (v - [v]\bar{v}) \right). \quad (\text{D15})$$

where  $\lambda^S$  and  $\lambda^v$  are the vectors of the Lagrange multipliers. The variations are then given by the following:

$$\partial_S : \Delta \bar{S} - \bar{\lambda}^S = 0, \quad (\text{D16})$$

$$\partial_{\bar{S}} : \Delta S - \lambda^S = 0, \quad (\text{D17})$$

$$\partial_v : 2\Delta v - \lambda^v = 0, \quad (\text{D18})$$

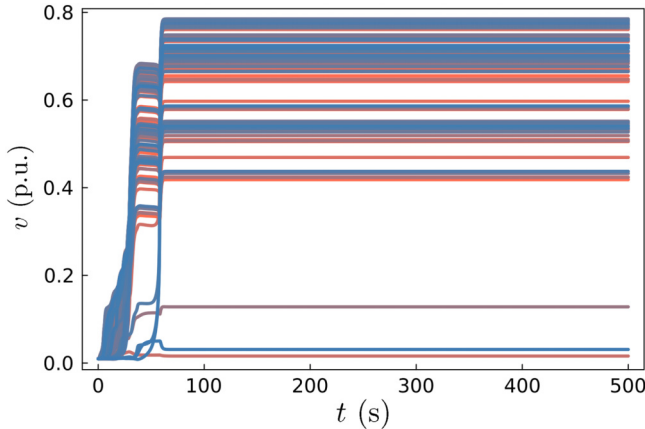


FIG. 7. An attempted black start of a system with 100 nodes.

$$\partial_v : [\bar{\lambda}^S]\bar{Y}\bar{v} - Y^T[\bar{v}]\lambda^S + [\lambda^v]\bar{v} = 0, \quad (\text{D19})$$

$$\partial_{\bar{v}} : \text{c.c.} \quad (\text{D20})$$

Multiplying the  $\partial_v$  variation with  $[v]$  and noting that we have  $[v]\bar{Y}\bar{v} = S$  and  $[v]Y^T[\bar{v}] = \bar{K}^T$ , we see that

$$[v]\partial_v : 0 = [\bar{\lambda}^S][S] - \bar{K}^T\lambda^S + [\lambda^v][v]\bar{v} \quad (\text{D21})$$

$$= [\Delta \bar{S}]S - \bar{K}^T\Delta S + 2[\Delta v]v \quad (\text{D22})$$

$$= \bar{\eta}^c. \quad (\text{D23})$$

Thus, with this quasilocal control (the control depends on the power imbalance at the neighbors and the state of the coupling on the edges),  $V$  is a Lyapunov function. If the set points satisfy the power-flow equations, then the system at the stable power flow has  $V = 0$  and is Lyapunov stable. The control law  $\eta^c$  always drives the system to the local minima of  $V$  on the physical manifold and these minima are fixed points, as the local minima satisfy  $\eta^c = 0$ .

- [1] ENTSO-E, High penetration of power electronic interfaced power sources and the potential contribution of grid forming converters (2020) [https://eepublicdownloads.entsoe.eu/clean-documents/Publications/SOC/High\\_Penetration\\_of\\_Power\\_Electronic\\_Interfaced\\_Power\\_Sources\\_and\\_the\\_Potential\\_Contribution\\_of\\_Grid\\_Forming\\_Converters.pdf](https://eepublicdownloads.entsoe.eu/clean-documents/Publications/SOC/High_Penetration_of_Power_Electronic_Interfaced_Power_Sources_and_the_Potential_Contribution_of_Grid_Forming_Converters.pdf).
- [2] Bundesnetzagentur, Genehmigung des Szenariorahmens 2021–2035 (2020) [https://www.netzentwicklungsplan.de/sites/default/files/paragraphs-files/Szenariorahmen\\_2035\\_Genehmigung\\_1.pdf](https://www.netzentwicklungsplan.de/sites/default/files/paragraphs-files/Szenariorahmen_2035_Genehmigung_1.pdf).
- [3] H Popella, T. Hennig, M. Kaiser, J. Massmann, L. Müller, and R. Pfeiffer, in *20th International Workshop on Large-Scale Integration of Wind Power into Power Systems As Well As on Transmission Networks for Offshore Wind Power Plants (WIW 2021)*, vol. 2021 (Institution of Engineering and Technology, London, 2021), p. 125.
- [4] T. Prevost and G. Denis, Migrate WP3: Control and operation of a grid with 100% converter-based devices, *Eur. Horiz.* **7923842** (2020).
- [5] J. Schiffer, R. Ortega, A. Astolfi, J. Raisch, and T. Sezi, Conditions for stability of droop-controlled inverter-based microgrids, *Automatica* **50**, 2457 (2014).

- [6] M. Colombino, D. Groß, and F. Dörfler, in *2017 IEEE 56th Annual Conference on Decision and Control (CDC), Melbourne, VIC, Australia* (IEEE, New York City, 2017), p. 5690.
- [7] D. Witthaut, F. Hellmann, J. Kurths, S. Kettemann, H. Meyer-Ortmanns, and M. Timme, Collective nonlinear dynamics and self-organization in decentralized power grids, *Rev. Mod. Phys.* **94**, 015005 (2022).
- [8] J. Machowski, J. W. Bialek, and J. R. Bumby, *Power System Dynamics: Stability and Control* (John Wiley & Sons, Chichester, UK, 2008), 2 ed. oCLC: ocn232130756.
- [9] S. Auer, K. Kleis, P. Schultz, J. Kurths, and F. Hellmann, The impact of model detail on power grid resilience measures, *Eur. Phys. J. Spec. Top.* **225**, 609 (2016).
- [10] R. Kogler, A. Plietzsch, P. Schultz, and F. Hellmann, Normal form for grid-forming power grid actors, *PRX Energy* **1**, 013008 (2022).
- [11] F. Milano, Complex frequency, *IEEE Trans. Power Syst.* **37**, 1230 (2022).
- [12] J. Machowski, Z. Lubosny, J. W. Bialek, and J. R. Bumby, *Power System Dynamics—Stability and Control* (John Wiley & Sons, Chichester, 2008).
- [13] IEEE. Part 118-1: Synchrophasor for power systems—measurements, *IEEE/IEC International Standard—Measuring Relays and Protection Equipment* (2018).
- [14] W. Zhong, G. Tzounas, M. Liu, and F. Milano, On-line inertia estimation of Virtual Power Plants, *Electr. Power Syst. Res.* **212**, 108336 (2022).
- [15] X. He, V. Häberle, and F. Dörfler, Complex-frequency synchronization of converter-based power systems, Preprint [ArXiv:2208.13860](https://arxiv.org/abs/2208.13860) (2022).
- [16] X. He, V. Häberle, I. Subotić, and F. Dörfler, Nonlinear stability of complex droop control in converter-based power systems, *IEEE Control Syst. Lett.* **7**, 1327 (2023).
- [17] G.S. Seo, M. Colombino, I. Subotic, B. Johnson, D. Groß, and F. Dörfler, in *2019 IEEE Applied Power Electronics Conference and Exposition (APEC), Anaheim, CA, USA* (IEEE, New York City, 2019), p. 561.
- [18] D. Moutevelis, J. Roldán-Pérez, M. Prodanovic, and F. Milano, Taxonomy of power converter control schemes based on the complex frequency concept, *IEEE Trans. Power Syst.* **39**, 1996 (2023).
- [19] R. Berner, T. Gross, C. Kuehn, J. Kurths, and S. Yanchuk, Adaptive dynamical networks, *Phys. Rep.* **1031**, 1 (2023).
- [20] J. Sawicki, *et al.*, Perspectives on adaptive dynamical systems, *Chaos: Interdiscip. J. Nonlinear Sci.* **33**, 071501 (2023).
- [21] R. Berner, S. Yanchuk, and E. Schöll, What adaptive neuronal networks teach us about power grids, *Phys. Rev. E* **103**, 042315 (2021).
- [22] K. Schmietendorf, J. Peinke, R. Friedrich, and O. Kamps, Self-organized synchronization and voltage stability in networks of synchronous machines, *Eur. Phys. J. Spec. Top.* **223**, 2577 (2014).
- [23] F. Hellmann, P. Schultz, P. Jaros, R. Levchenko, T. Kapitaniak, J. Kurths, and Y. Maistrenko, Network-induced multistability through lossy coupling and exotic solitary states, *Nat. Commun.* **11**, 592 (2020).
- [24] B. Charlet, J. Lévine, and R. Marino, On dynamic feedback linearization, *Syst. Control. Lett.* **13**, 143 (1989).
- [25] J. Coulson, J. Lygeros, and F. Dörfler, in *18th European Control Conference (ECC), Naples, Italy* (IEEE, New York City, 2019), p. 307.
- [26] Z. M. Zhai, M. Moradi, L. W. Kong, B. Glaz, M. Haile, and Y. C. Lai, Model-free tracking control of complex dynamical trajectories with machine learning, *Nat. Commun.* **14**, 143 (2023).
- [27] E. Sontag, *Mathematical Control Theory: Deterministic Finite Dimensional Systems* (Springer, New York City, 1998).
- [28] P. M. Pardalos and V. Yatsenko, *Optimization and Control of Bilinear Systems* (Springer, New York City, 2008).
- [29] R. R. Mohler and W. J. Kolodziej, An overview of bilinear system theory and applications, *IEEE Trans. Syst. Man. Cybern.* **10**, 683 (1980).
- [30] L. M. Pecora and T. L. Carroll, Master stability functions for synchronized coupled systems, *Phys. Rev. Lett.* **80**, 2109 (1998).
- [31] R. Berner, S. Vock, E. Schöll, and S. Yanchuk, Desynchronization transitions in adaptive networks, *Phys. Rev. Lett.* **126**, 028301 (2021).
- [32] A. Isidori, *Nonlinear Control Systems* (Springer, London, 1995).
- [33] E. D. Sontag, A “universal” construction of Artstein’s theorem on nonlinear stabilization, *Syst. Control Lett.* **13**, 117 (1989).
- [34] M. Andreasson, H. Sandberg, D. V. Dimarogonas, and K. H. Johansson, in *2012 IEEE 51st IEEE Conference on Decision and Control (CDC), Maui, HI, USA* (IEEE, New York City, 2012), p. 2077.
- [35] J. Schiffer, F. Dörfler, and E. Fridman, Robustness of distributed averaging control in power systems: Time delays & dynamic communication topology, *Automatica* **80**, 261 (2017).
- [36] A. Büttner, A. Plietzsch, M. Anvari, and F. Hellmann, A framework for synthetic power system dynamics, *Chaos: Interdiscip. J. Nonlinear Sci.* **33**, 083120 (2023).
- [37] A. Büttner and F. Hellmann, Control-Lyapunov Function for Networks, Zenodo (2023). <https://doi.org/10.5281/zenodo.10245703>
- [38] P. Schultz, J. Heitzig, and J. Kurths, A random growth model for power grids and other spatially embedded infrastructure networks, *Eur. Phys. J. Spec. Top.* **223**, 2593 (2014).
- [39] dena, dena-Verteilnetzstudie: Ausbau- und Innovationsbedarf der Stromverteilnetze in Deutschland bis 2030, <https://www.dena.de/newsroom/publikationsdetailansicht/pub/dena-verteilnetzstudie-ausbau-und-innovationsbedarf-der-stromverteilnetze-in-deutschland-bis-2030/>.
- [40] J. Egerer, DIW Berlin: Open Source Electricity Model for Germany (ELMOD-DE), [https://www.diw.de/de/diw\\_01.c.528929.de/publikationen/data\\_documentation/2016\\_0083/open\\_source\\_electricity\\_model\\_for\\_germany\\_\\_elmod-de.html](https://www.diw.de/de/diw_01.c.528929.de/publikationen/data_documentation/2016_0083/open_source_electricity_model_for_germany__elmod-de.html).
- [41] F. Milano, *Power System Modelling and Scripting*, Power Systems (Springer, 2010).
- [42] C. Rackauckas and Q. Nie, DifferentialEquations.jl – A performant and feature-rich ecosystem for solving differential equations in Julia, *J. Open. Res. Softw.* **5**, 15 (2017).
- [43] J. Bezanson, A. Edelman, S. Karpinski, and V. B. Shah, JULIA: A fresh approach to numerical computing, *SIAM Rev.* **59**, 65 (2017).